PNAS RESEARCH ARTICLE | CELL BIOLOGY

TET3-mediated DNA oxidation is essential for intestinal epithelial cell response to stressors

Edward A. Gonzalez[a,1], Yue Liu[a,1], Dahui Wang[a,1], Maciej Jeziorek[a], Sheila Bandyopadhyay[a], Anjana Rao[b,c,d], Nan Gao[a,e,2,3], and Jean-Pierre Etchegaray[a,e,3]

Edited by Carl Nathan, Weill Medical College of Cornell University, New York, NY; received January 9, 2023; accepted July 5, 2023

DNA methylation functions as a repressive epigenetic mark that can be reversed by the Ten-eleven translocation (TET) family of DNA dioxygenases that sequentially oxidize 5-methylcytosine into 5-hydroxymethylcytosine (5hmC), 5-formylcytosine (5fC), and 5-carboxylcytosine (5caC). Both 5fC and 5caC can be excised by DNA base-excision repair factors leading to unmodified cytosines. TET enzymes were recently implicated as potential risk factors for inflammatory bowel disease (IBD), but the contribution of TET-mediated DNA oxidation to intestinal homeostasis and response to environmental stressors are unknown. Here, we show prominent roles of TET3 in regulating mouse intestinal epithelial differentiation and response to luminal stressors. Compared with wild-type littermates, mice with intestinal epithelial cell-specific ablation of *Tet3* (*Tet3*$^{\Delta IEC}$) demonstrated a decreased transcriptome involved in innate immune response, Paneth cell differentiation, and epithelial regeneration. *Tet3*^{IEC} mice exhibited an elevated susceptibility to enteric pathogen infection that is correlated with a decreased epithelial 5hmC abundance. Infection of human enterocytes or mice with the pathogenic bacteria acutely increased 5hmC abundance. Genome-wide 5hmC profiling revealed a shift of genomic enrichment of 5hmC toward genes involved in activating Notch, Wnt, and autophagy pathways. Furthermore, chemical stressor dextran sulfate sodium (DSS) represses epithelial 5hmC abundance in a temporal fashion, and *Tet3*^{IEC} mice exhibited increased susceptibility to DSS experimental colitis with reduced regenerative capacity. TET3 is a critical regulator of gut epithelial DNA methylome and transcriptome, especially in response to luminal stressors, for the maintenance of tissue homeostasis.

epigenetic | cell biology | immunology | inflammation | intestinal epithelia

Significance

Recent single-cell transcriptomic studies predicted TET enzymes, which are DNA dioxygenases capable of changing the epigenome, among risk genes in ulcerative colitis patients. However, the role of TET-mediated epigenetic reprogramming affecting intestinal epithelial physiology under conditions of homeostasis and in response to stressors remains largely unclear. Here, we described an essential role for TET3-mediated DNA production of 5hmC to protect intestinal epithelial integrity from pathogenic infection and chemical stressors by promoting the expression of genes involved in Notch and Wnt signaling pathways.

Epigenetic mechanisms contributing to intestinal homeostasis and disease susceptibility remain poorly understood (1). Changes to DNA methylation profiles in intestinal epithelial cells (IECs) have been observed upon colonization by commensal microbiota (2). Methylated DNA functions as a repressive mark for gene expression and is pivotal for cell fate commitment in embryonic development (3). DNA methylation at specific genomic loci has been shown to be critical for the acquisition and maintenance of cellular identity and function in mammals (3). However, there remains a paucity of experimental data on how DNA methylation patterns are dynamically regulated in response to intestinal luminal stressors and participate in mucosal innate response. DNA methylation is catalyzed by DNA methyltransferases (DNMT), generating 5-methylcytosine (5mC) (4). In mammals, in addition to passive removal of methyl groups during DNA replication, active demethylation can be catalyzed by the Ten-eleven translocation (TET) family of enzymes, TET1, TET2, and TET3 (4). TET enzymes are DNA dioxygenases that can sequentially oxidize 5mC into 5-hydroxymethylcytosine (5hmC), 5-formylcytosine (5fC), and 5-carboxylcytosine (5caC) (4). These DNA oxidations can function as DNA demethylation intermediates, as thymine DNA glycosylase (TDG) can further excise 5fC and 5caC through a DNA base-excision repair (BER) mechanism resulting in unmodified cytosines (4). TET-mediated DNA oxidations are enriched at genomic loci with high transcription factor occupancy in embryonic stem cells (5).

A human scRNA-seq study predicted TET enzymes among new risk genes in ulcerative colitis patients (6). However, the role of TET enzymes in IEC physiology remains unknown. Based on scRNA-seq data (7), we found that *Tet3* is highly expressed in mouse IECs comparing to *Tet1* and *Tet2*. Here, we genetically ablated *Tet3* in mouse intestinal epithelia and observed a global reduction of 5hmC in *Tet3*Δ^{IEC} mouse IECs that exhibited an altered epithelial differentiation program at steady states. These mice also showed elevated susceptibilities to challenges by enteric pathogenic bacteria or barrier-disrupting chemical stressor. Genomic profiling of 5hmC in human enterocytes before and after pathogenic bacterial infection revealed that infection triggered a significant genomic

Author affiliations: [a]Department of Biological Sciences, Rutgers University-Newark, Newark, NJ 07102; [b]Division of Signaling and Gene Expression, La Jolla Institute for Immunology, La Jolla, CA 92037; [c]Sanford Consortium for Regenerative Medicine, La Jolla, CA 92037; [d]Department of Pharmacology and Moores Cancer Center, University of California, La Jolla, CA 92093; and [e]Rutgers Cancer Institute of New Jersey, New Brunswick, NJ 08901

Author contributions: N.G. and J.-P.E. designed research; E.A.G., Y.L., D.W., M.J., and S.B. performed research; A.R. contributed new reagents/manuscript editing; and J.-P.E. wrote the paper.

The authors declare no competing interest.

This article is a PNAS Direct Submission.

[1]E.A.G., Y.L., and D.W. contributed equally to this work.

[2]N.G. is the co-corresponding author.

[3]To whom correspondence may be addressed. Email: ngao@rutgers.edu or jeanpierre.etchegaray@rutgers.edu.

This article contains supporting information online at https://www.pnas.org/lookup/suppl/doi:10.1073/pnas.2221405120/-/DCSupplemental.

Published September 5, 2023.

redistribution of 5hmC to genes involved in regulating epithelial regeneration and growth signaling pathways. Our results suggest that TET3 is an essential DNA dioxygenase responsible for an epigenetic reprogramming that allows proper epithelial cell differentiation and response to barrier-disrupting luminal stressors.

Results

Genetic Ablation of *Tet3* in the Intestinal Epithelium Altered the Mature Mouse IEC Population. To determine the expression levels of the three mouse *Tet* genes, we analyzed the mouse IEC single-cell RNA sequencing (scRNA-seq) data reported by Haber et al. (7) (Fig. 1*A*). We found that compared to *Tet1* (Fig. 1*B*) and *Tet2* (Fig. 1*C*), *Tet3* is the most abundantly expressed *Tet* gene in the IECs (Fig. 1*D*). Notably, *Tet3* is expressed in diverse epithelial cell types, most notably the enterocytes and Tuft cells (Fig. 1*E*), which regulate intestinal barrier and immune functions (8, 9). Immunohistochemistry for TET3 confirmed its expression along the crypt-villus axis with villus IECs showing higher abundances (Fig. 1*F*). Immunohistochemistry for 5hmC illustrated strong epithelial cell nuclear staining in both crypt and villus compartments (Fig. 1*G*).

As TET3 may be the major TET enzymes in mouse IECs, we developed IEC-specific *Tet3* knockout mice ($Tet3\Delta^{IEC}$) by crossing $Tet3^{Flox}$ mice (10) to *Villin-Cre* driver to investigate the role of TET3 in IEC function. At steady states, $Tet3\Delta^{IEC}$ mice do not show overt abnormality by body weight or intestinal histology. Immunohistochemistry revealed a significant reduction of lysozyme-

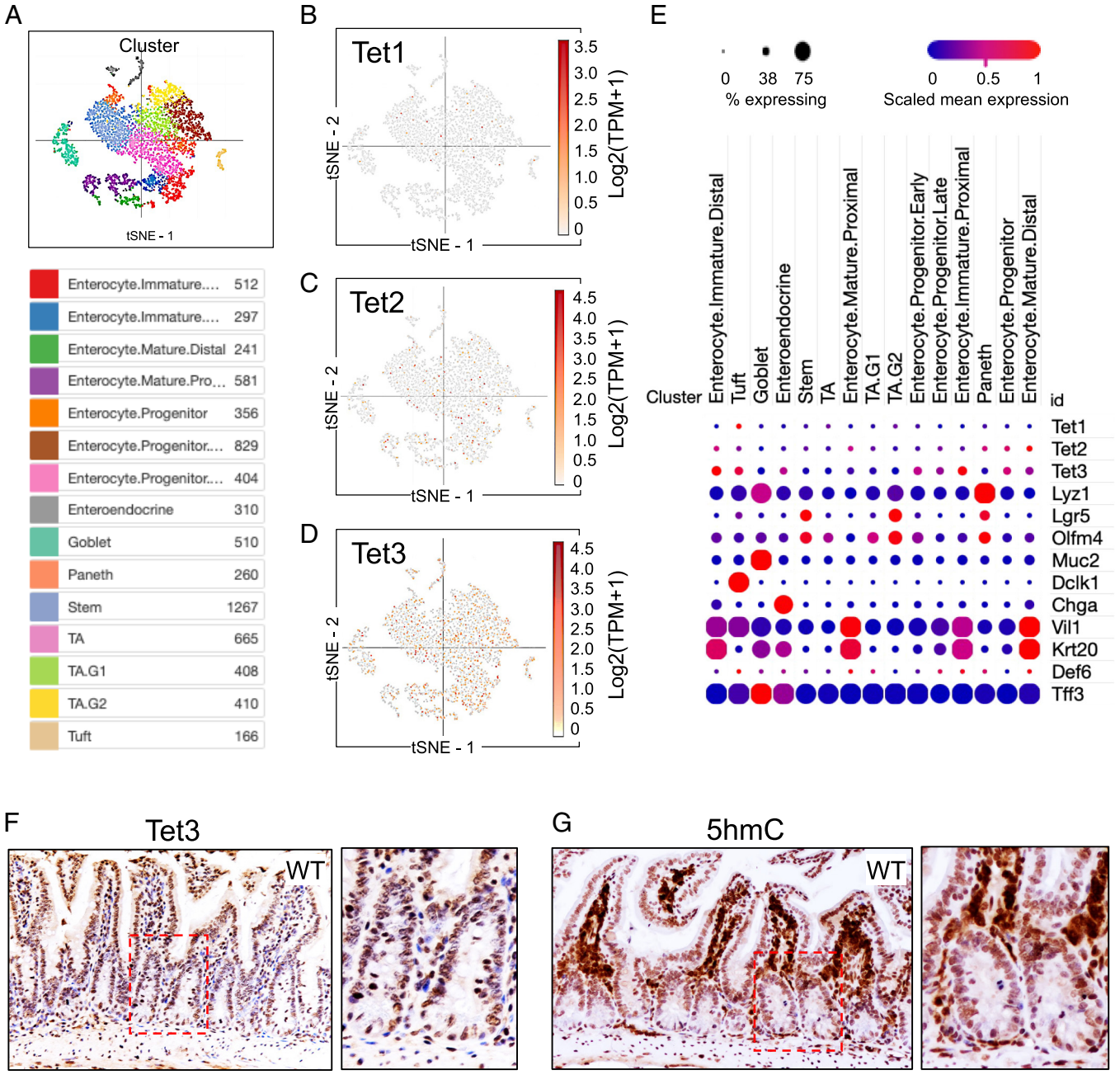

Fig. 1. *Tet3* is more abundantly expressed in IECs than *Tet1* and *Tet2*. Gene expression analysis was performed using the mouse intestinal epithelial single-cell RNA dataset of Haber et al. (7). (*A*) tSNE of whole mouse small IECs (7,216 cells) showed different IEC clusters. (*B–D*) Mapping *Tet1*, *Tet2*, and *Tet3* on IECs by tSNE analysis. (*E*) Dot plots show cell type–specific expressional abundance of Tet3 across various IEC cell types. Larger dots indicate higher expression compared to smaller dots. (*F* and *G*) Immunohistochemistry (IHC) staining showing the distribution of TET3 and 5hmC in the crypt-villus axis of WT mice.

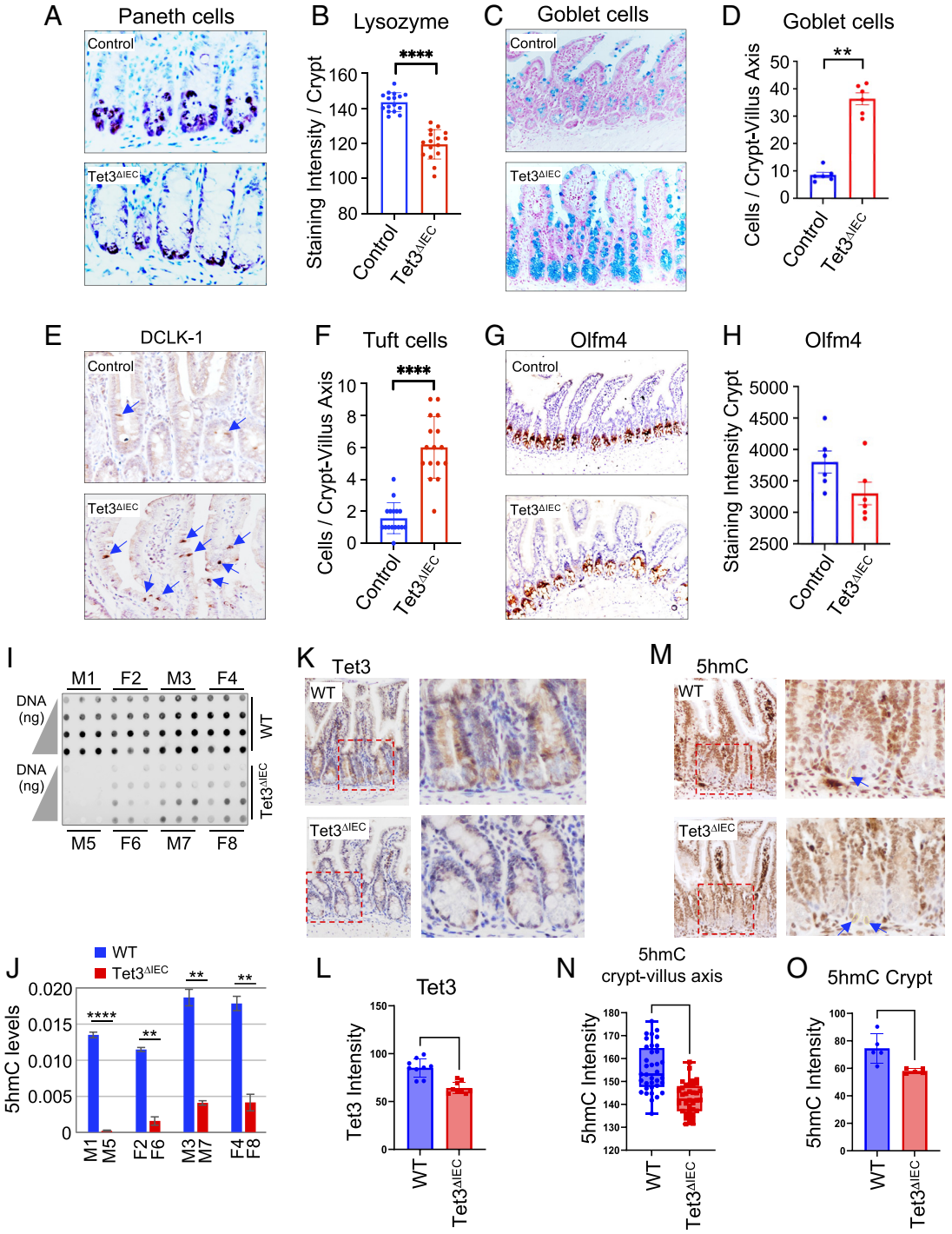

Fig. 2. *Tet3*$^{\Delta IEC}$ mouse intestinal epithelia show altered epithelial cell composition. (*A* and *B*) Lysozyme staining and quantification to assess Paneth cells. (*C* and *D*) Alcian blue staining and quantification to assess goblet cells. (*E* and *F*) DCLK-1 staining and quantification to assess Tuft cells. (*G* and *H*) Olfm4 staining and quantification to assess crypt base columnar stem cells. Statistical analysis was performed five to six mice per genotype (**$P < 0.01$ and ****$P < 0.0001$, error bars represent SEM). (*I*) Dot blot analysis showing a global decrease of 5hmC abundance in genomic DNA from the *Tet3*$^{\Delta IEC}$ mice ileum compared to WT littermates under homeostasis. (*J*) 5hmC quantification from of the WT and *Tet3*$^{\Delta IEC}$ mice ileum (n = 4 per genotype, **$P < 0.01$, ****$P < 0.0001$, error bars represent SEM). (*K* and *L*) TET3 staining (IHC) and quantification in the crypt-villus axis of WT and *Tet3*$^{\Delta IEC}$ mice (n = 9 per genotype, ****$P < 0.0001$). (*M* and *O*) 5hmC staining (IHC) of WT and *Tet3*$^{\Delta IEC}$ mice and quantification in the crypt-villus axis (n =30 per genotype, ****$P < 0.0001$) and quantification in crypt (n = 5 per genotype, **$P < 0.0088$).

expressing Paneth cells, when compared to control littermates (Fig. 2 *A* and *B*). This reduction of Paneth cells was accompanied by ~fourfold expansion in the number of goblet and Tuft cells in *Tet3Δ*^{IEC} ileum (Fig. 2 *C*–*F*). Interestingly, the number of *Olfm4* expressing intestinal stem cells (ISCs) was modestly reduced in *Tet3Δ*^{IEC} ileum (Fig. 2 *G* and *H*). These changes in epithelial cell composition were not due to the presence of *Tet3*^{Flox} or *Villin-Cre* allele alone, or due to cage effects, as littermates with no *Villin-Cre* or with *Villin-Cre* alone were examined as controls in our analysis. These data suggest that TET3 deficiency causes an alteration in the IEC composition in homeostasis.

Since TET enzymes are DNA dioxygenases targeting the oxidation of 5mC into 5hmC (4), we determined the abundances of 5hmC in *Tet3Δ*^{IEC} mouse small intestinal epithelia by dot blot

analysis. Under homeostatic conditions, we found a radical decrease of 5hmC abundance in *Tet3Δ*^{IEC} compared to wild-type (WT) mouse ileum ($P < 0.01$, Fig. 2 *I* and *J*), suggesting that TET3 may play a predominant role compared to other TET enzymes in IECs (Fig. 1 *D* and *E*). Immunohistochemistry for TET3 and for 5hmC suggested decreased abundances along the crypt-villus axis in *Tet3Δ*^{IEC} mice compared to controls (Fig. 2 *K–O* and *SI Appendix*, Fig. S2 *A* and *B*). Since 5hmC is usually enriched at actively transcribed genes (5), the decreased 5hmC in *Tet3*-deficient IECs suggest that TET3-mediated DNA oxidation may regulate the expression of specific genes involved in IEC functions such as epithelial differentiation or tissue maintenance.

Decreased Growth Signaling and Innate Immune Response Gene Networks in *Tet3*$^{\Delta IEC}$ Mice. To identify genes whose expression is affected by *Tet3* deletion in IECs, we performed bulk RNA-Seq analysis using ileal RNAs extracted from control and *Tet3Δ*^{IEC} littermates (n = 5 each genotype, both genders). Principal component and differential gene expression analysis showed transcriptomic differences including 631 significantly decreased and 960 increased transcripts in the *Tet3Δ*^{IEC} mouse ileum (Fig. 3 *A* and *B*). Heatmap and pathway analysis revealed reduced gene networks involved in growth signaling, antimicrobial response, immune defense, and cellular stemness (Fig. 3*C*). Gene ontology (GO) analysis by Enrichr cataloged the most significantly reduced pathways in *Tet3Δ*^{IEC} mice included type I interferon responses (e.g., *Ifitm2, Ifitm3, Irf7, Ifit1,* and *Gbp2*), Wnt and Notch signaling (e.g., *Dll1, Dll4, Wnt3*, and *Wnt9b*), antimicrobial response (e.g., *Lyz1, Lyz2, Reg3b,* and *Reg3g*), and cellular stemness (e.g., *Olfm4, Lgr4, Lgr5,* and *Sox9*) (Fig. 3 *C* and *D* and Dataset S1). Immunohistochemistry for HES1, a Notch signaling target and effector (11), showed a significant reduction in *Tet3Δ*^{IEC} mouse IECs, comparing to controls (Fig. 3 *F* and *G*). Interestingly, the most significantly increased genes revealed by Enrichr are involved in cellular glucuronidation, a major detoxification pathway for endo- and xenobiotics (e.g., *Ugt1a10, Ugt1a5, Ugt1a9,* and *Ugt1a8*), and epithelial development (e.g., *Hey2*, *Snai1*, *Pax8*, *Pou3f3*, *Pkhd1, Slc4a7, Rilpl1,* and *Pdzd7*) (Fig. 3*E* and Dataset S2). Among them, *Hey2* and *Snai1* are noted as transcription factors downstream of Notch signaling, which affects differentiation of Paneth cells (12). Thus, loss of *Tet3* in mouse intestinal epithelia altered the transcriptomic networks involved in epithelial growth and innate defense.

***Tet3*$^{\Delta IEC}$ Mice Have Increased Susceptibility to Enteric Pathogen Infection.** The changed expression of innate immune response genes suggests that TET3 may be required for IECs to respond to luminal stressors such as invasive pathogens. We therefore analyzed 5hmC abundances in the ileum and colon of WT mice at different time points after *Salmonella* infection. We found a significant enrichment of 5hmC abundance 6 h after *Salmonella* infection in the ileum (Fig. 4 *A–C*) and a similar enrichment in the colon only 3 h after infection (Fig. 4 *D–F*), suggesting that infection acutely promoted TET enzyme activity.

Next, we challenged WT and *Tet3Δ*^{IEC} mice with 10^8 colony-forming unit (CFU) *Salmonella typhimurium* per mouse, following a standard protocol with an oral streptomycin pretreatment. Infected *Tet3Δ*^{IEC} mice, of both genders, showed greater body weight loss than littermate WT mice (Fig. 4*G*). Experiments were terminated at 5 days after infection (dpi), as *Tet3Δ*^{IEC} mice showed 20% body weight loss. Scoring of colonic inflammation revealed a significantly increased mucosal inflammation in *Tet3Δ*^{IEC} mice (Fig. 4 *H* and *I*), consistent with an increased systemic *Salmonella* dissemination to the spleen and liver in these *Tet3Δ*^{IEC} animals (Fig. 4 *J* and *K*)**.** We measured global 5hmC contents in intestinal epithelia of infected mice 5 dpi, and found a diminished 5hmC abundance in *Tet3Δ*^{IEC} mice (Fig. 4 *L* and *M*), suggesting that the other TET enzymes did not effectively compensate TET function after infection. These data suggest that TET3-mediated 5hmC regulation plays a critical role in the host response to gut pathogen infection.

Pathogen Infection in Human Enterocytes Induces TET-Mediated DNA Oxidation and Genomic 5hmC Redistribution. TET3 is highly enriched in mouse enterocytes (Fig. 1 *D* and *E*), which are the major cell type of infection by *Salmonella*. It is unknown whether pathogenic infection of human enterocytes may affect TET-mediated DNA oxidation. We thus infected the human enterocyte cell line Caco2-BBE with *S. typhimurium.* Caco2-BBE is a Caco2 subclone (13) that develops brush border with enriched expression of Villin that facilitates *Salmonella* infection (14). Upon *Salmonella* infection of confluent Caco2-BBE monolayer, we observed a temporal and significant increase of 5hmC abundance within the first 10 min followed by a 3-h time course of infection (Fig. 5 *A* and *B*).

To investigate whether infection drives TET-mediated DNA oxidation to specific gene networks, thereby modifying the cellular transcriptome in response to infection, we infected Caco2-BBE monolayers with *S. typhimurium* for 3 h and then performed 5hmC DIP (DNA immunoprecipitation)-sequencing (hMeDIP-seq) on uninfected and infected cells (Dataset S3). Principal component analysis revealed the differential clustering between uninfected and infected Caco2 cells (*SI Appendix*, Fig. S1*A*). We observed a global redistribution of 5hmC at various genomic regions including enhancers, introns, exons, promoters, and CpGs (Fig. 5 *C* and *D* and Datasets S4 and S5). Gain and loss of 5hmC were observed at 8,761 and 15,493 gene loci, respectively (Fig. 5*E* and *SI Appendix*, Fig. S1*B*). Notably, the genes that acquired a gain in 5hmC are involved in the activation of Wnt/β-catenin (*CBP*, *SMARCA4*, and *KIF3B*), Notch (*RBPJ*, *PRKCI*, and *ZMIZ1*), or autophagy (*ITGB4*, *ING1*, and *UBXN2A*) pathways (Fig. 5 *F* and *G*). These pathways have been shown to be activated in IECs as part of the innate immune defense program (15–17). Genome-wide analysis has associated 5hmC enrichment with high transcription factor occupancy at genomic regions including active enhancers, thereby enrichment of 5hmC on the above genes suggested a potential positive regulation for their expression (18). Interestingly, we found that the gain of 5hmC for these genes occurs at enhancer regions (Fig. 5 *C* and *G*). The genes exhibiting a loss of 5hmC after pathogenic infection are related to cell migration and cell-cell adhesion, negative regulation of cell proliferation, and Fc-gamma receptor signaling, which is involved in cytotoxicity and phagocytosis during microbial infection (19) (*SI Appendix*, Fig. S1*D*).

We next investigated whether gain of 5hmC correlates with activation of gene expression in the context of infection. We performed a correlation analysis using our 5hmC genome-wide results with RNA-seq data from the human 3D enteroid model system infected with *Salmonella* (20). Sixty-two genes enriched for 5hmC were increased in response to *Salmonella* infection (Fig. 6*A* and Dataset S6). Strikingly, 11 out of these 62 genes (18%) are direct activators of the Wnt/β-catenin pathway, while six of them (e.g., CBP, *BRG1*, *AXIN1*, *MSI2*, *ZMIZ1*, and *MSN*) are also involved in promoting the Notch pathway (Fig. 6*B* and *SI Appendix*, Fig. S1*C*). Consistent with an enriched 5hmC occupancy, we validated that these genes (*RBPJ, SENP2,* and *CREBBP*) were significantly increased in Caco2-BBE cells after *Salmonella* infection (Fig. 6*C*). Furthermore, we established a *TET2*-knockdown Caco2-BBE cell line, where both *TET1* and

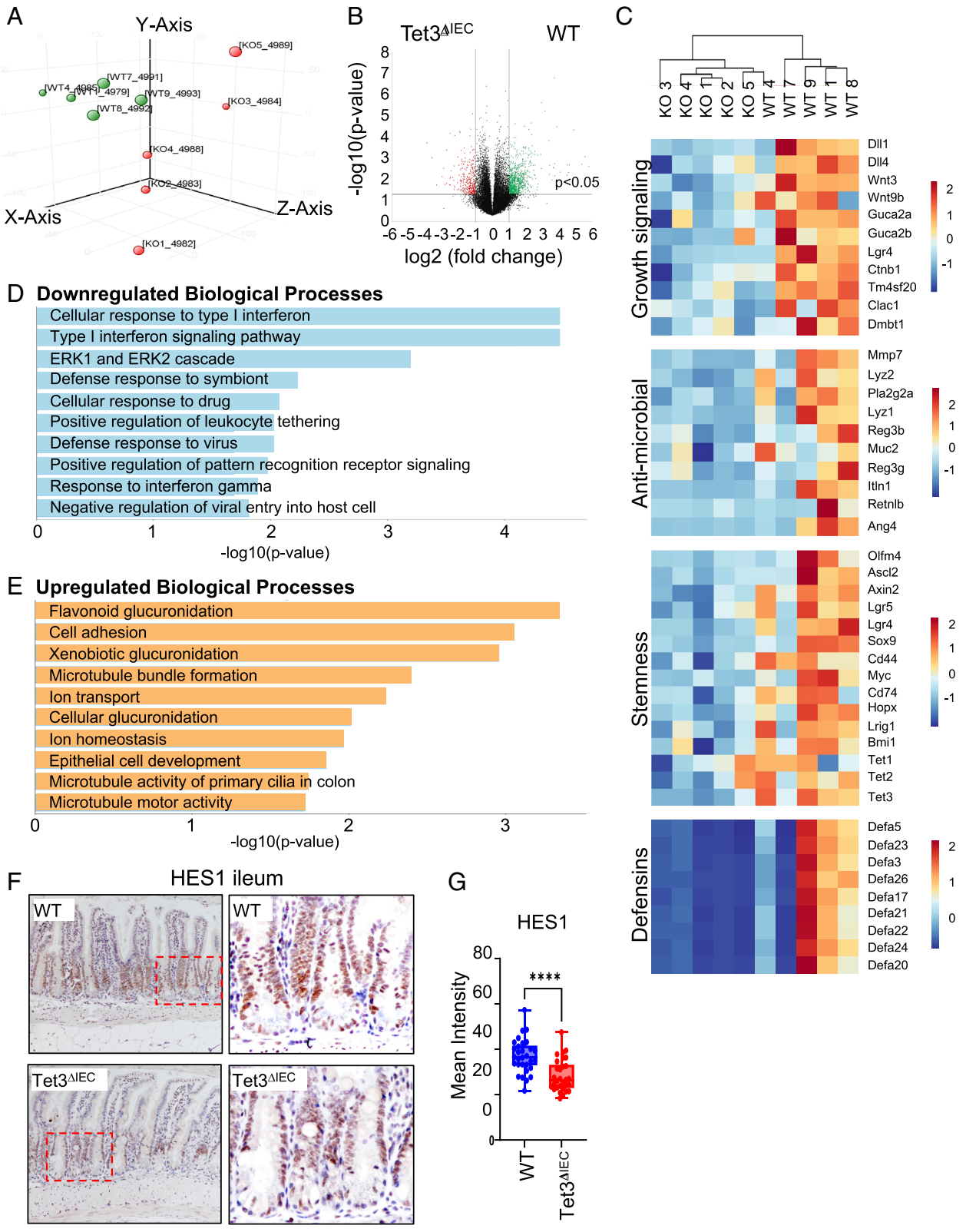

Fig. 3. Altered transcriptome in the *Tet3*$^{\Delta IEC}$ mouse ileum. (*A*) Bulk RNA sequencing was performed on the control and *Tet3*$^{\Delta IEC}$ mouse ileum. Principal components analysis showing clustering of control versus *Tet3*$^{\Delta IEC}$ mice. (*B*) Differential gene expression analysis in control versus *Tet3*$^{\Delta IEC}$ mice (n = 5 per each genotype). (*C*) Heatmap showing downregulation of genes involved in growth signaling, antimicrobial response, innate defense, and stemness in *Tet3*$^{\Delta IEC}$ mice. (*D*) GO (Enrichr) showing down-regulated cellular pathways involved in innate immune response in *Tet3*$^{\Delta IEC}$ mice. (*E*) GO (Enrichr) showing up-regulated cellular pathways involved in detoxification and epithelial cell development in *Tet3*$^{\Delta IEC}$ mice. (*F* and *G*) Hes1 staining (IHC) of WT and *Tet3*$^{\Delta IEC}$ mice and quantification of the crypt- villus axis (n = 30 per genotype, ****$P < 0.0001$).

TET3 were also significantly down-regulated supporting our previous finding suggesting an autoregulatory mechanism among the TET family of enzymes (21). We found that the expression of these 5hmC-enriched genes was significantly down-regulated in *TET2*-deficient Caco2-BBE cells (Fig. 6*D*). These data linked 5hmC enrichment with positive transcriptional activation during infection,

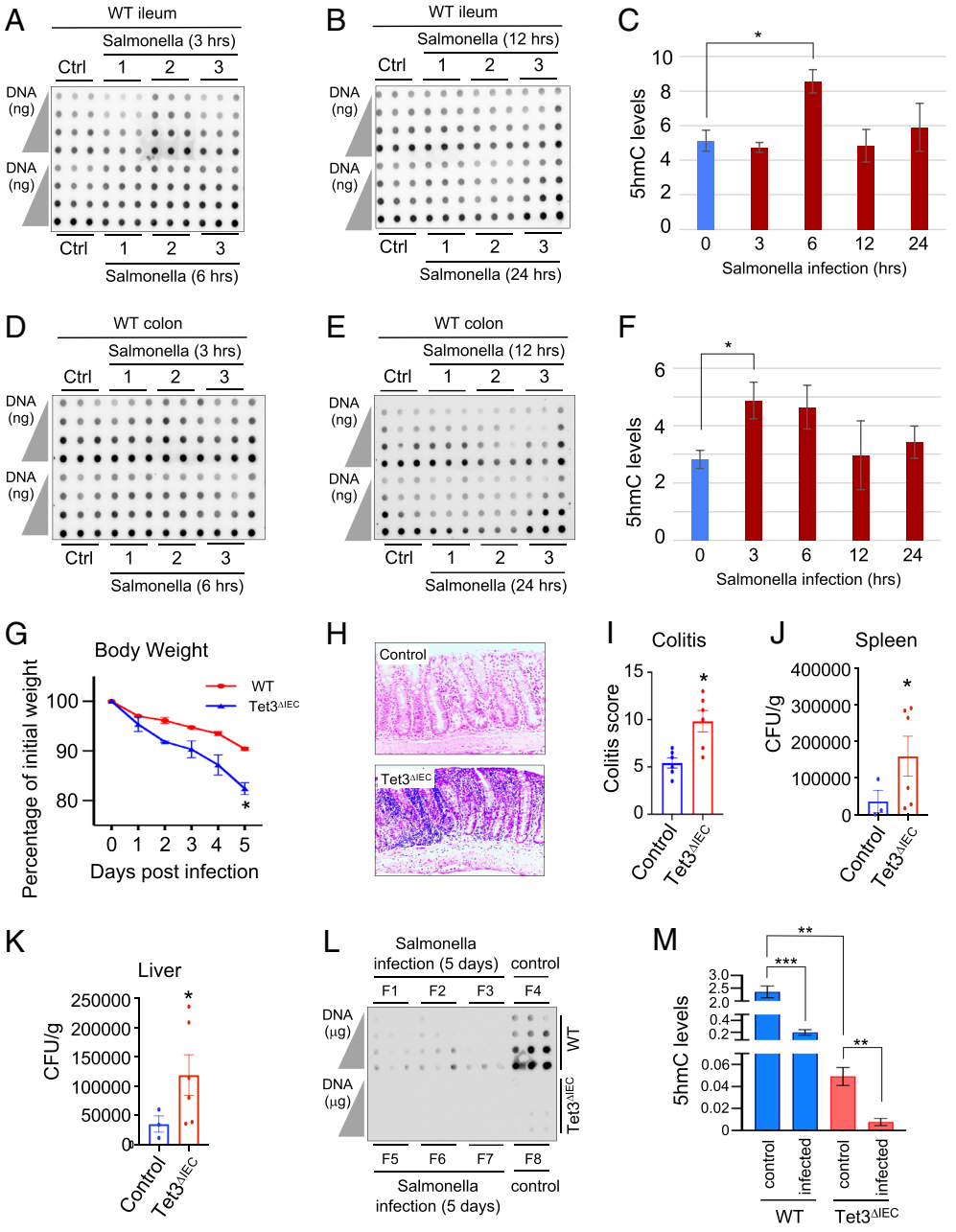

Fig. 4. *Tet3*$^{\Delta IEC}$ mice are susceptible to *S. typhimurium* infection. (*A–C*) Dot blot analysis and quantification showing time-dependent augmented 5hmC in genomic DNA from the ileum of WT mice at 0, 3, 6, 12, and 15 h after Salmonella infection (n = 3, **P* < 0.02). (*D–F*) Dot blot analysis and quantification showing time-dependent augmented 5hmC in genomic DNA from the colon of WT mice at 1, 3, 6, 12, and 24 h after *Salmonella* infection (n = 3, **P* < 0.05). (*G*) Body weight changes after *Salmonella* infection of WT and *Tet3*$^{\Delta IEC}$ mice (four to six mice per genotype). (*H* and *I*) Histopathology and scoring of colonic inflammation of infected mice at 5 dpi. (*J* and *K*) *Salmonella* CFUs in the spleen and liver at 5 dpi. (*L* and *M*) Dot blot analysis and quantification showing decreased 5hmC abundance in genomic DNA from WT mice ileum after 5 d of *Salmonella* infection, which is nearly undetectable in *Tet3*$^{\Delta IEC}$ mice ileum (n = 3, **P* < 0.05, ***P* < 0.01, and *****P* < 0.0001, error bars represent SEM).

suggesting that TET-mediated DNA oxidation may be an integral epigenetic program of enterocytes in response to pathogen infection.

***Tet3*$^{\Delta IEC}$ Mice Show Exacerbated DSS-Induced Colitis.** IECs expose to various luminal stressors including chemicals. To investigate whether TET-mediated DNA modification changes in response to chemical stressors, we measured colonic 5hmC abundance following dextran sulfate sodium (DSS) treatment of WT mice through drinking water. Notably, colonic 5hmC remained constant at early time points but became significantly reduced 7 d after the treatment (Fig. 7 *A* and *B*). We next challenged WT and *Tet3Δ*^{IEC} mice with 3% DSS through drinking water for 7 d followed by regular water to allow recovery. Both *Tet3Δ*^{IEC} and control littermates exhibited body weight loss in the first 7 d, while *Tet3Δ*^{IEC} mice showed virtually no recovery following the switch to regular water (Fig. 7*C*). Control mice showed a recovery at day 9. We terminated the experiments on day 12 when some *Tet3Δ*^{IEC} mice showed more than 20% body weight loss. Upon killing, *Tet3Δ*^{IEC} mice showed significantly shorter colons (Fig. 7 *D* and *E*), severer inflammation scored on epithelial damage, and immune cell infiltration (Fig. 7 *F* and *G*). Measuring of colonic 5hmC showed a diminished 5hmC in *Tet3Δ*^{IEC} colons comparing to WT mice (Fig. 7 *H* and *I*). Immunohistochemistry suggested

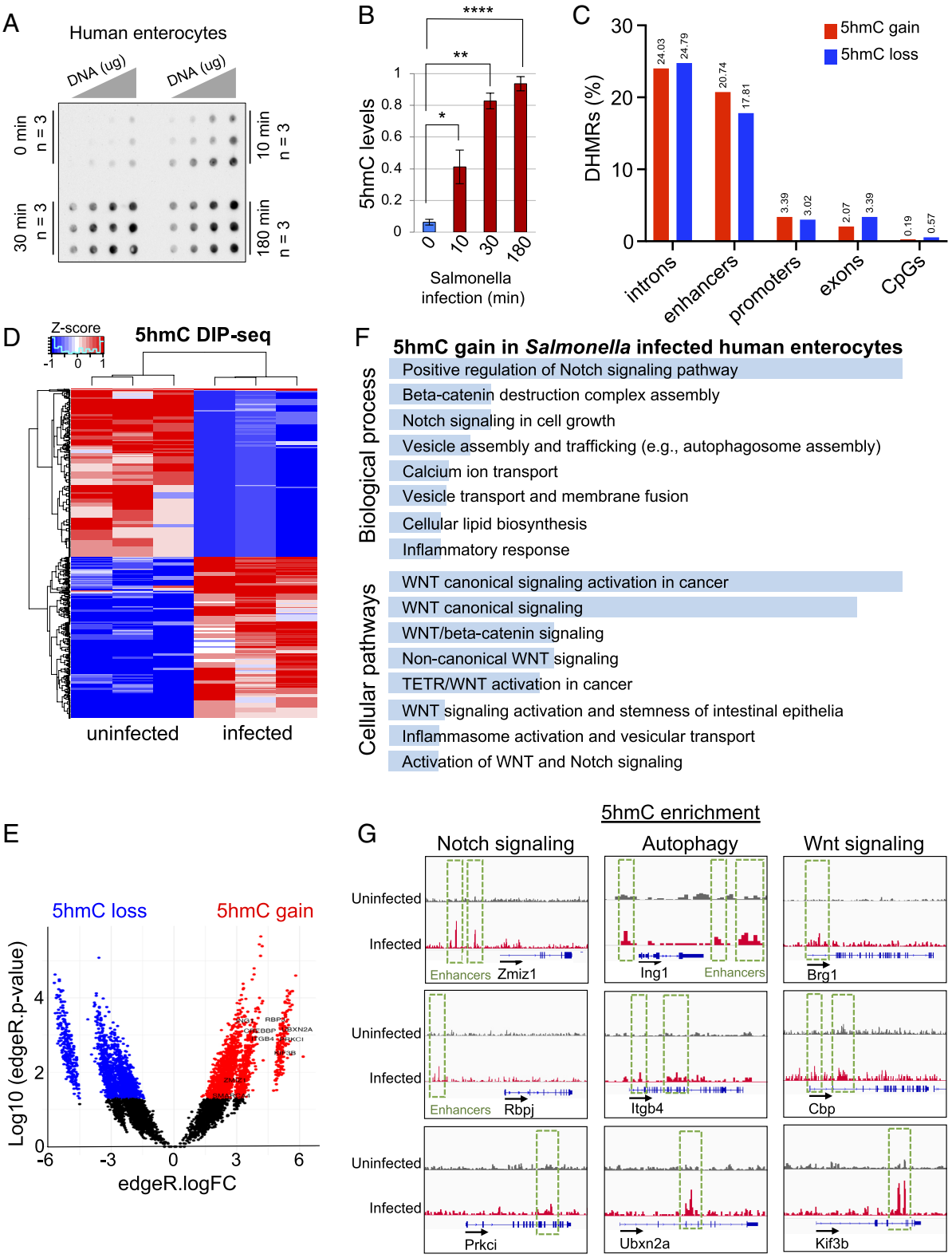

Fig. 5. Genomic distribution of 5hmC in response to pathogenic infection. (*A* and *B*) Dot blot analysis and quantification showing augmented 5hmC in genomic DNA from human enterocytes (Caco-2 cells) in a time course–dependent manner after *Salmonella* infection (n = 3, **P* < 0.05, ***P* < 0.01, and *****P* < 0.0001, error bars represent SEM). 5hmC DIP-seq analysis in uninfected and *Salmonella*-infected Caco2 cells (n = 3). (*C*) Gain and loss of 5hmC at different genomic regions including enhancers, promoters, introns, exons, and CpGs. (*D*) Heatmap from 5hmC DIP-seq (*E*) Volcano plot showing the gain and loss of 5hmC at specific genes. (*F*) Biological and cellular pathway analysis by Enrichr. (*G*) 5hmC enrichment on specific genes involved in Notch, autophagy, and Wnt signaling using Integrative Genomics Viewer.

a significantly reduced HES1-positive colonic epithelial cells in DSS-treated *Tet3Δ*^{IEC} colons (Fig. 7 *J* and *K*), accompanied by a similarly reduced epithelial proliferation marked by Ki67 cells (Fig. 7 *L* and *M*). Collectively, these data indicate that TET3 has a protective role against chemical stressors in addition to enteric pathogen.

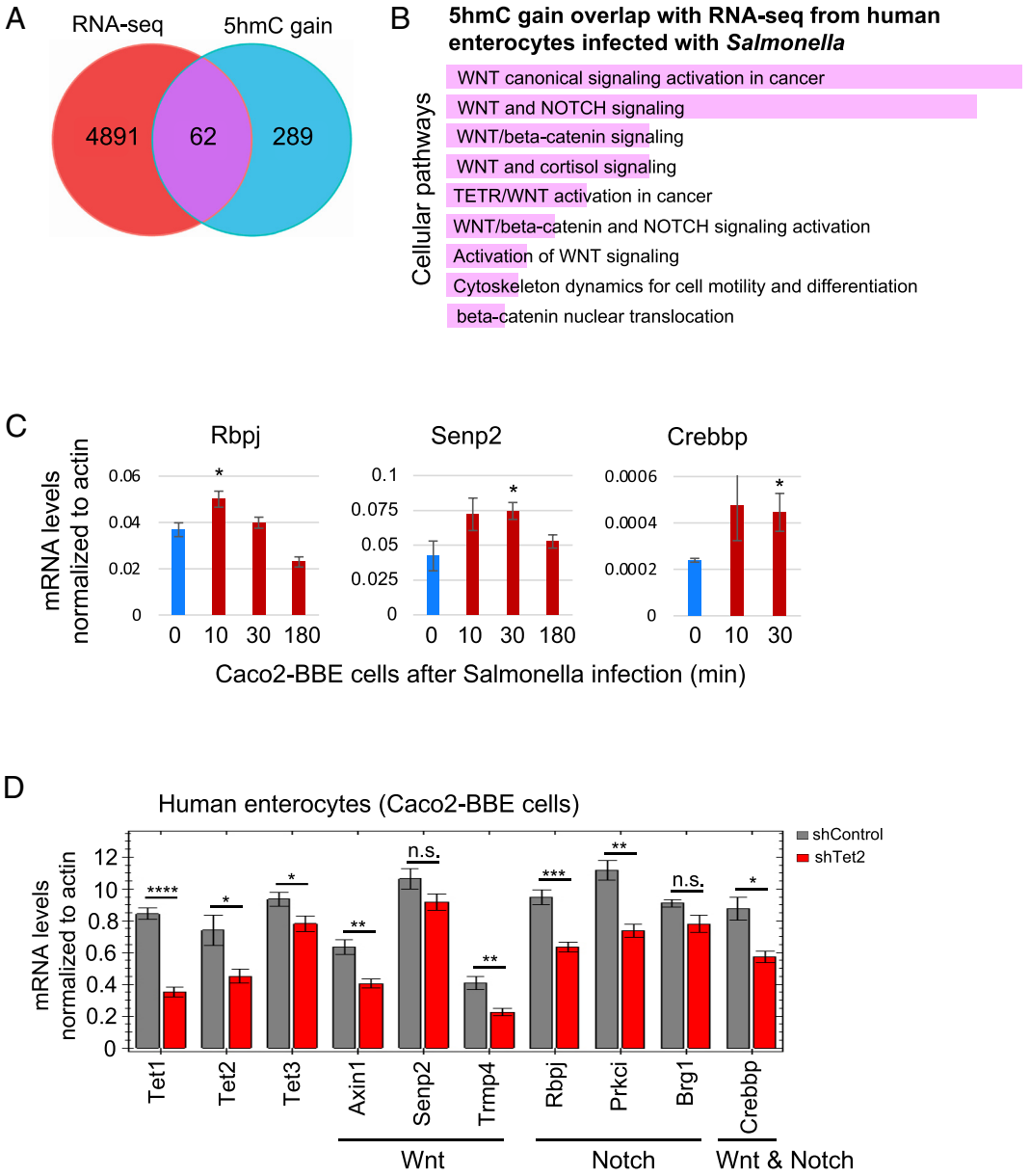

Fig. 6. 5hmC linked to Notch and Wnt signaling pathways. (*A*) Venn diagram showing the correlation between 5hmC DIP-seq and RNA-seq from Barrila et al. (20). (*B*) Cellular pathway analysis by Enrichr from the overlapped genes in the Venn diagram on (*A*). (*C*) qRT-PCR of Caco2-BBE-infected with *S. typhimurium* for genes targets up-regulated in 5hMeDIP involved with Notch and WnT signaling (n = 8, **P* < 0.05). (*D*) qRT-PCR of Caco2-BBE knocked down for *TET2* for the TET enzymes and genes involved with Notch and WnT signaling (n = 4, **P* < 0.05, ***P* < 0.01, ****P* < 0.001, *****P* < 0.0001, and n.s. = non-significant)

Discussion

TET-dependent DNA oxidations are an integral part of the epigenome and can function as intermediates of DNA demethylation (4). However, it remains unknown if DNA oxidations control cell fate changes in the intestinal epithelia under homeostasis or stress conditions. We previously showed that TET-mediated DNA oxidation is required for the maintenance of stemness in ESCs (21). However, the impact of TET-mediated DNA oxidations on mature IEC response to luminal stressors and their downstream molecular pathways remain not fully determined. A previous study by Kim et al. (22) focused on ISCs, in which they found that *Tet1* was the mostly abundantly expressed *Tet* gene. Haber et al. scRNA-seq survey of mouse IECs (7) suggests that TET3 is the most broadly expressed TET enzyme, especially in multiple clusters of enterocytes. We validated at the protein level that TET3 is expressed in IECs along the crypt-villus axis, with higher abundance in the villus epithelial cells. Of note, *Tet1*-deficient mice are growth-retarded and show partial postnatal lethality, indicating *Tet1*'s critical role in stem cell renewal or maintenance (22). In contrast, adult *Tet3*-deficient mice in our study are viable and fertile, even though the intestines have an altered IEC population. Interestingly, ISC genes with high levels of hydroxymethylation are strongly associated with Wnt signaling and *Tet1*-deficient intestines had reduced Wnt target genes that correlate with lower 5hmC (22). Consistently, our study independently demonstrated reduced Wnt and Notch pathway genes in *Tet3*-deficient intestines through bulk RNA-seq. Our 5hmC DIP-seq analysis of human enterocyte cells also pointed to TET-regulated hydroxymethylation at Wnt and Notch pathway genes in steady state and in response to infection. Inhibition of Notch led to goblet cell hyperplasia or metaplasia (23, 24). A reduced Notch signaling in *Tet3*-deficient mice is consistent with the observed goblet cell hyperplasia in these mice. Thus, TET1-mediated DNA hydroxymethylation may play a dominant role in

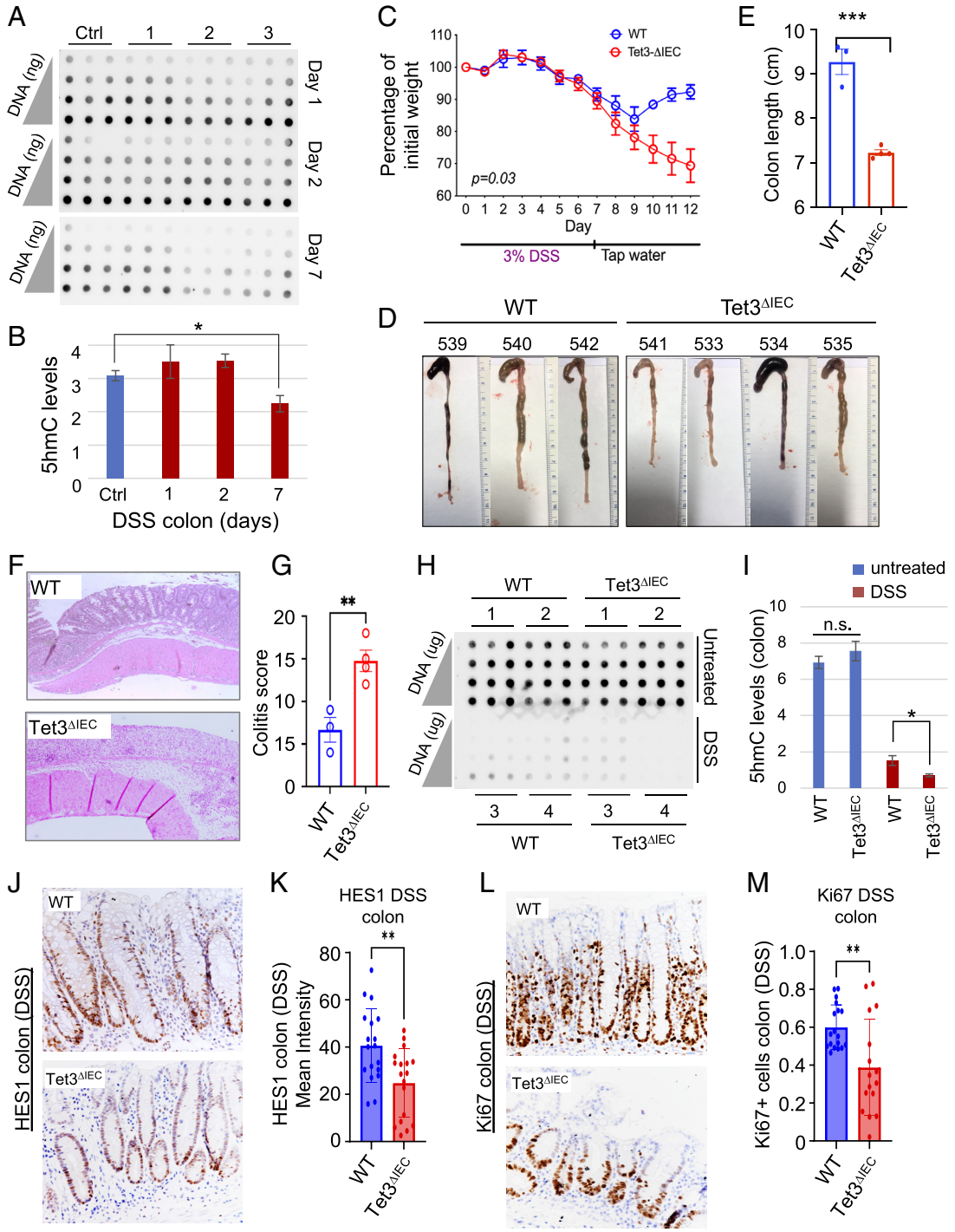

Fig. 7. *Tet3*$^{\Delta IEC}$ mice failed to recover from DSS-induced colitis. (*A* and *B*) Dot blot analysis and quantification showing a time-dependent decrease in 5hmC in genomic DNA from the colon of WT mice at days 1, 2, and 7 after DSS treatment (n = 3, *$P < 0.05$). (*C*) Body weight changes during DSS-induced colitis development in control and *Tet3*$^{\Delta IEC}$ littermates (n > 3 per genotype). (*D* and *E*) Colon length and gross morphology of control and *Tet3*$^{\Delta IEC}$ mice. (*F* and *G*) Histopathology and colitis scores of DSS-treated WT and *Tet3*$^{\Delta IEC}$ mouse colons at 5 dpi. (*H* and *I*) Dot blot analysis and quantification showing a global decrease of 5hmC abundance in genomic DNA from WT mice following 7 d of DSS treatment followed by 5 d of recovery (n = 6 experimental replicates, *$P < 0.05$). (*J* and *K*) 1 staining (IHC) of the colon from WT and *Tet3*$^{\Delta IEC}$ mice treated with DSS and quantification of mean intensity in the colon (n = 18, **$P < 0.0033$). (*L* and *M*) Ki67 staining (IHC) of the colon from WT and *Tet3*$^{\Delta IEC}$ mice treated with DSS and quantification of mean intensity in the colon (n = 16, **$P < 0.0034$).

the ISC compartment whereas TET3 may be essential for the differentiation of mature epithelial cells and for response to luminal stressors.

Previous and our studies collectively suggest that TET1 and TET3 may share common regulatory targets such as the Wnt pathway. Alternatively, as our previous and current data suggested interregulation among different TET enzymes (21), the observed 5mhC changes could be a cumulative effect of multiple TET enzymes. Kim et al did not examine intestinal phenotypes under chemical or pathogen-challenged conditions (22). Our study showed temporal changes in global 5hmC abundance and a dynamic shift of gene-specific TET-mediated DNA modification in response to stressors. Our finding that *Tet3Δ*^{IEC} mice are susceptible to pathogenic infection and chemical-induced oxidative stress may shed light on the prediction of TET2 as one of the new risk genes for human ulcerative colitis (UC) (6). Interestingly, our stable *TET2*

knockdown Caco2 cells had reduced expression of *TET1*, *TET3*, and multiple Wnt and Notch pathway genes found in our 5hmC DIP-seq analysis. More recently, TET2-mediated maintenance of 5hmC at promoters and enhancers was shown to stimulate demethylation and activation of stemness genes during somatic cellular reprogramming to generate induced pluripotent stem cells (25). Since DNA oxidations can function as intermediates for DNA demethylation (26), the upregulation of Wnt signaling genes enriched for 5hmC that we observed in response to *Salmonella* infection may be caused by DNA demethylation. The cells may use this mechanism to promote growth and tissue repair.

At the molecular level, we found a global redistribution of 5hmC within the epigenetic landscape of human enterocytes in response to pathogenic infection that resulted in the upregulation of *CBP* (*CREBBP*) and *BRG1* (*SMARCA4*) genes, which encode for major chromatin regulators capable of interacting with beta-catenin to promote activation of genes targeted by the Wnt signaling pathway (27, 28). CBP is a histone acetyltransferase that facilitates gene expression by creating a transcriptionally permissive epigenetic landscape and BRG1 is a core subunit of the Adenosine triphosphate (ATP)-dependent chromatin remodeling complex SWI/SNF involved in the control of innate immune transcriptional programs (29) (30). Plausibly, this 5hmC-dependent epigenetic reprogramming promotes the expression of master epigenetic regulators such as CBP and BRG1 to synergize the activation of specific gene networks in response to stressors such as microbial infection. Overall, our data support a role for TET3 as an essential stress-responsive epigenetic regulator to reprogram the transcriptome of IECs in response to stressors such as pathogenic infection and DSS-mediated oxidative stress. These data open the door for future research to investigate how TET enzymes are capable of sensing environmental challenges, how luminal stressors modulate TET enzyme functions, and how loss of Paneth cells in $Tet3\Delta^{IEC}$ mice might contribute to the exacerbated phenotypes during infection and chemical injury.

Materials and Methods

Mice. The *Tet3flox/flox* and *Villin-Cre* mice have been described previously (10, 31, 32). All animals were bred in-house and maintained in specific pathogen-free conditions at Rutgers University. All animal experiments were conducted in accordance with the animal protocol approved by Institutional Animal Care and Use Committee (IACUC) at Rutgers University. The control and knockout mice were housed in sterilized cages in a room held at a controlled temperature (20 to 22 °C) with controlled relative humidity (45 to 55%) and 12/12 h light/dark cycles at the Rutgers Animal Care Facility. All the animals had free access to water and diet throughout the experiment. The description of *S. typhimurium* infection and DSS treatment can be found in *SI Appendix, Materials and Methods*.

Cell Culture. The human Caco2-BBE cells were obtained from American Type Culture Collection (ATCC). Caco2- cells were grown in DMEM (Sigma D5671) supplemented with 20% Fetal Bovine Serum (FBS), 1× MEM Non-essential Amino Acid Solution (Sigma M7145), 10 mM N-2-hydroxyethylpiperazine-N-2-ethane sulfonic acid (HEPES) solution (Sigma H0887), 1 mM sodium pyruvate solution (Sigma S8636), 2 mM L-glutamine solution (Sigma G7513), antibiotics (100 I.U./mL- penicillin, 100 µg/mL –streptomycin, Sigma P4333), and 100 µg/mL Primocin (InvivoGen, ant-pm-2). To generate a stable cell line, Caco2 were transduced with commercially available lentivirus encoding shRNA for *TET2* (GeneCopoeia, Cat. HSH064384) at MOI of 25 with 8 µg/mL polybrene overnight. Treatment of Caco2-BBE with *S. typhimurium* can be found in *SI Appendix, Materials and Methods*.

Immunohistochemistry of Mouse Intestinal Tissues. Immunohistochemical (IHC) tissue analysis was performed as previously described (12). Briefly, phosphate-buffered formalin-fixed, paraffin-embedded mouse intestinal tissue sections were dewaxed by heat and xylene treatment, followed by rehydration of tissue through soaked in gradients of ethanol ranging from 100 to 50% followed by deionized water. Endogenous peroxide activity was quenched by immersing slides into 0.3% hydrogen peroxide solution with methanol for 40 min at room temperature The tissue slides were then subjected to antigen-retrieval in citrate buffer (0.1 M citric acids, pH 6.0) for 15 min, during which tissue slides were soaked in preboiled citrate buffer and heated using a commercial microwave. The tissue slides were then cooled down through a water bath, washed, and blocked for 1 h with 2% appropriate animal serum in Phosphate-buffered saline (PBS) at room temperature. Primary antibody incubation was performed overnight at 4 °C. The primary antibodies used were as follows: anti-lysozyme (BioGenex, Cat No. PU024-5UP) at 1:200 dilution. After primary antibody treatment, the slides were washed with PBS and incubated with horseradish peroxidase (HRP)-conjugated goat anti-rabbit IgG (Vector Laboratories Inc., Cat No. BA-1000) at 1:200 dilution for 1 h at room temperature. Following the secondary antibody treatment, the slides were washed with PBS and developed using the standard substrate detection of DAB (Vector Laboratories Inc., Cat No. SK-4100). Tissue slides were mounted using Cytoseal-60 (ThermoFisher Scientific, Cat No. 8310-4). Quantification of all images can be found in *SI Appendix, Materials and Methods*.

The RNA and DNA genome-wide experiments and analyses and dot blot methods can be found in *SI Appendix, Materials and Methods*.

Data, Materials, and Software Availability. Next-generation sequencing data have been deposited in the Gene Expression Omnibus (GEO) repository, accession number GSE241808 (33).

ACKNOWLEDGMENTS. We thank Dr. Edward Bonder and the Advanced Imaging Core Facility in the Department of Biological Sciences at Rutgers School of Arts and Sciences-Newark, for imaging assistance. This work is supported by NIH awards: R01AT010243, R01DK132885 and R01DK119198 to N.G, R21AI167079 to J-P.E. and N.G., R35CA210043 to A.R, and E.A.G. is supported by NIGMS G-Rise training grant 5T32GM140951.

1. H. Gehart, H. Clevers, Tales from the crypt: New insights into intestinal stem cells. *Nat. Rev. Gastroenterol. Hepatol.* **16**, 19–34 (2019).
2. I. Ansari *et al.*, The microbiota programs DNA methylation to control intestinal homeostasis and inflammation. *Nat. Microbiol.* **5**, 610–619 (2020).
3. Z. D. Smith, A. Meissner, DNA methylation: Roles in mammalian development. *Nat. Rev. Genetics* **14**, 204–220 (2013).
4. C. J. Lio *et al.*, TET methylcytosine oxidases: New insights from a decade of research. *J. Biosci.* **45**, 21 (2020).
5. W. A. Pastor *et al.*, Genome-wide mapping of 5-hydroxymethylcytosine in embryonic stem cells. *Nature* **473**, 394–397 (2011).
6. C. S. Smillie *et al.*, Intra- and inter-cellular rewiring of the human colon during ulcerative colitis. *Cell* **178**, 714–730.e722 (2019).
7. A. L. Haber *et al.*, A single-cell survey of the small intestinal epithelium. *Nature* **551**, 333–339 (2017).
8. V. Snoeck, B. Goddeeris, E. Cox, The role of enterocytes in the intestinal barrier function and antigen uptake. *Microbes Infect.* **7**, 997–1004 (2005).
9. T. E. Billipp, M. S. Nadjsombati, J. von Moltke, Tuning tuft cells: New ligands and effector functions reveal tissue-specific function. *Curr. Opin. Immunol.* **68**, 98–106 (2021).
10. J. Kang *et al.*, Simultaneous deletion of the methylcytosine oxidases Tet1 and Tet3 increases transcriptome variability in early embryogenesis. *Proc. Natl. Acad. Sci. U.S.A.* **112**, E4236–E4245 (2015).
11. S. J. Liang, X. G. Li, X. Q. Wang, Notch signaling in mammalian intestinal stem cells: Determining cell fate and maintaining homeostasis. *Curr. Stem Cell Res. Ther.* **14**, 583–590 (2019).
12. S. Yu *et al.*, Paneth cell multipotency induced by notch activation following injury. *Cell Stem Cell* **23**, 46–59.e45 (2018).
13. M. D. Peterson, M. S. Mooseker, Characterization of the enterocyte-like brush border cytoskeleton of the C2BBe clones of the human intestinal cell line, Caco-2. *J. Cell Sci.* **102**, 581–600 (1992).
14. N. Lhocine *et al.*, Apical invasion of intestinal epithelial cells by *Salmonella typhimurium* requires villin to remodel the brush border actin cytoskeleton. *Cell Host Microbe* **17**, 164–177 (2015).
15. S. Haq, J. Grondin, S. Banskota, W. I. Khan, Autophagy: Roles in intestinal mucosal homeostasis and inflammation. *J. Biomed. Sci.* **26**, 19 (2019).
16. S. Jati, T. R. Sarraf, D. Naskar, M. Sen, Wnt signaling: Pathogen incursion and immune defense. *Front Immunol.* **10**, 2551 (2019).
17. Y. Obata *et al.*, Epithelial cell-intrinsic Notch signaling plays an essential role in the maintenance of gut immune homeostasis. *J. Immunol.* **188**, 2427–2436 (2012).
18. A. Tsagaratou *et al.*, Dissecting the dynamic changes of 5-hydroxymethylcytosine in T-cell development and differentiation. *Proc. Natl. Acad. Sci. U.S.A.* **111**, E3306–E3315 (2014).
19. T. Castro-Dopico, M. R. Clatworthy, IgG and Fcgamma receptors in intestinal immunity and inflammation. *Front Immunol.* **10**, 805 (2019).

20. J. Barrila *et al.*, Spaceflight analogue culture enhances the host-pathogen interaction between Salmonella and a 3-D biomimetic intestinal co-culture model. *Front Cell Infect. Microbiol.* **12**, 705647 (2022).
21. J. P. Etchegaray *et al.*, The histone deacetylase SIRT6 controls embryonic stem cell fate via TET-mediated production of 5-hydroxymethylcytosine. *Nat. Cell Biol.* **17**, 545–557 (2015).
22. R. Kim, K. L. Sheaffer, I. Choi, K. J. Won, K. H. Kaestner, Epigenetic regulation of intestinal stem cells by Tet1–mediated DNA hydroxymethylation. *Genes Dev.* **30**, 2433–2442 (2016).
23. J. Milano *et al.*, Modulation of notch processing by gamma-secretase inhibitors causes intestinal goblet cell metaplasia and induction of genes known to specify gut secretory lineage differentiation. *Toxicol. Sci.* **82**, 341–358 (2004).
24. J. H. van Es *et al.*, Notch/gamma-secretase inhibition turns proliferative cells in intestinal crypts and adenomas into goblet cells. *Nature* **435**, 959–963 (2005).
25. J. L. Sardina *et al.*, Transcription factors drive Tet2–mediated enhancer demethylation to reprogram cell fate. *Cell Stem Cell* **23**, 905–906 (2018).
26. X. Yue, A. Rao, TET family dioxygenases and the TET activator vitamin C in immune responses and cancer. *Blood* **136**, 1394–1401 (2020).
27. A. Hecht, K. Vleminckx, M. P. Stemmler, F. van Roy, R. Kemler, The p300/CBP acetyltransferases function as transcriptional coactivators of beta-catenin in vertebrates. *EMBO J.* **19**, 1839–1850 (2000).
28. N. Barker *et al.*, The chromatin remodelling factor Brg-1 interacts with beta-catenin to promote target gene activation. *EMBO J.* **20**, 4935–4943 (2001).
29. N. Shiama, The p300/CBP family: Integrating signals with transcription factors and chromatin. *Trends Cell Biol.* **7**, 230–236 (1997).
30. J. Gatchalian, J. Liao, M. B. Maxwell, D. C. Hargreaves, Control of stimulus-dependent responses in macrophages by SWI/SNF chromatin remodeling complexes. *Trends Immunol.* **41**, 126–140 (2020).
31. F. el Marjou *et al.*, Tissue-specific and inducible Cre-mediated recombination in the gut epithelium. *Genesis* **39**, 186–193 (2004).
32. B. B. Madison *et al.*, Cis elements of the villin gene control expression in restricted domains of the vertical (crypt) and horizontal (duodenum, cecum) axes of the intestine. *J. Biol. Chem.* **277**, 33275–33283 (2002).
33. Rutgers University, TET-mediated DNA oxidation sustains intestinal homeostasis and protects from stressors. Gene Expression Omnibus GEO. https://www.ncbi.nlm.nih.gov/geo/query/acc.cgi?acc=GSE241808. Deposited 29 August 2023.